References

Benesi, H., and Hildebrand, J. (1949), *J. Amer. Chem. Soc. 71*, 2703.

Bergman, E., and Pullman, B., Ed. (1969), *Jerusalem Symp. Quantum Chem. Biochem. 1.*

Bhattacharya, R., and Basu, S. (1958), *Trans. Faraday Soc. 54*, 1286.

Caspary, W., Lesko, S., Lorentzen, R., and Ts'o, P. (1973), *Abstr., 17th Annu. Meeting Biophys. Soc., Columbus, Ohio*, 26.

Hoffmann, H., Lesko, S., and Ts'o, P. (1970), *Biochemistry 9*, 2594.

Inomata, M., and Nagata, C. (1972), *GANN 63*, 119.

Jeftic, L., and Adams, R. (1970), *J. Amer. Chem. Soc. 92*, 1332.

Keuchler, E., and Der Kosch, J. (1966), *Z. Naturforsch. B, 21*, 209.

Lesko, S., Hoffmann, H., Ts'o, P., and Maher, V. (1971), *Progr. Mol. Subcell. Biol. 2*, 347.

Lesko, S., Ts'o, P., and Umans, R. (1969), *Biochemistry 8*, 2291.

Lohrmann, R., and Khorana, H. (1964), *J. Amer. Chem. Soc. 86*, 4188.

Mulliken, J. (1950), *J. Amer. Chem. Soc. 72*, 600.

Mulliken, J. (1951), *J. Chem. Phys. 19*, 514.

Nagata, C., Inomata, M., Kodama, M., and Tagashira, Y. (1968), *GANN 59*, 289.

Pullman, B., Pullman, A., Umans, R., and Maigret, B. (1969), *Jerusalem Symp. Quantum Chem. Biochem. 1*, 325.

Rochlitz, J. (1967), *Tetrahedron 23*, 3043.

Szent-Györgyi, A., Isenberg, I., and Baird, S. (1960), *Proc. Nat. Acad. Sci. U. S. 46*, 1444.

Wilk, M., and Girke, W. (1969), *Jerusalem Symp. Quantum Chem. Biochem. 1*, 91.

Ultracentrifugal Study of Polydisperse and Paucidisperse Biological Systems Using Capillary Microcells†

Julio C. Pita* and Francisco J. Müller

ABSTRACT: An ultracentrifugal technique based in the transport method to study polydisperse and/or paucidisperse biological systems is reported. The sedimentation cells used were either capillary tubes holding about 4 μl of dilute solutions or small cellulose tubes of 0.8-ml capacity. The methodology was used in connection with a Model L Beckman Spinco ultracentrifuge and an SW 50.1 swinging bucket rotor. Some of the concepts and procedures applied were presented in a previous publication (Pita, J. C., and Müller, F. J. (1972), *Anal. Biochem. 47*, 395). Three modes of approach were studied: (a) successive aliquot extractions along the tube length; (b) analysis of integral concentrations in the centripetal segment of the cell; and (c) centrifugations at different speed settings. The distribution function, $g(s)$, is obtained as a second derivative curve of the experimental concentrations found across the boundary gradient region. The plateau region was also studied and recognized to yield, when the experimental data are adequately plotted, straight line plots, with slope close to unity. The theory is easily extended to the case of paucidisperse systems. Boundary spreading due to diffusion is distinguished from polydispersity spreading. Several biological specimens, human serum albumin, preparations of a proteoglycan complex and its subunit, as well as a hypothetical trigonometric example, were used to analyze the possibilities of the technique. Results are found in good agreement with those obtained with conventional ultracentrifugal methods as reported in the literature.

The study of physical properties related to centrifugal heterogeneity shown by systems composed of a monomer in the presence of one or more polymers (paucidisperse systems) or those constituted by a polydisperse or continuous distribution of molecular weights is important for the correct understanding of biological mechanisms.

A previous publication (Pita and Müller, 1972) described a technique, based in the transport method, that permits the evaluation of sedimentation coefficients using only a few nanograms of biological principles. Purity of the sample was not required as long as the contaminants did not interfere with the analytical assay used. However, only single, monocomponent, solutions were considered in detail. It is the purpose of the current report to describe a methodology which, applying some of the concepts and experimental procedures included in the above-mentioned publication, allows the ultracentrifugal study of paucidisperse and polydisperse biological systems as well.

The exact shape and extent of the sedimenting boundary were, advantageously, of no relevance in the determination of sedimentation coefficients by the transport method (Pita and Müller, 1972). All measurements to that purpose were conducted in the plateau region, the boundary itself being considered as an ideal sharp demarcation without loss of mathematical rigor. In the present work, however, it is precisely the size, shape, and extent of the boundary that has to be studied, since according to Baldwin (1954) "the boundary gradient

† From the Department of Medicine and Orthopaedic Surgery, University of Miami School of Medicine and the Veterans Administration Hospital, Miami, Florida 33152. *Received January 29, 1973.* This research was supported in part by Grant AM-018662 from the National Institutes of Health, U. S. Public Health Service, the U. S. Veterans Administration Part I research grant, Florida Orthopaedic Society, and by the Helen and Michael Schaffer Foundation.

curve is itself a distribution curve" (of sedimentation coefficients).

The simplest approach to the study of the boundary region by a nonoptical method would be to analyze successive aliquots along the tube length after centrifugation is completed. If these concentration values are then plotted against their corresponding radial coordinates a curve is obtained similar to those found with conventional optical techniques. Difficulties arise, however, when thin capillary tubes are introduced as centrifugation cells. In this case the smallness of the volumes hinders the use of successive aliquot extractions, which produce significant boundary distortion. An alternative procedure, consistent with ultramicro sample volumes, is to analyze the concentration of solution contained within a tube length H as measured from the meniscus, x_m, to a partition plane at x (Figure 1A). With a group of these "integral" concentrations, obtained by centrifuging simultaneously several capillary cells having different H lengths, a plot is constructed from which a schlieren-type curve can be derived.

The technique of centrifuging several microcells might still be insufficient in cases where the distribution range of sedimentation coefficients is too widely spread about a given peak value. The available lengths of capillary cells could be too small to cover the range of H values needed. This infrequent situation can be solved by introducing the product $\omega^2 t$ (quadratic angular speed by centrifugation time) as another variable in the centrifugal study. Watanabe *et al.* (1954) have given an approximate solution to this approach by using a fixed partition macrocell (H = constant) and translating the various supernatant concentrations, coming from different $\omega^2 t$ runs, into a distribution curve of sedimentation coefficients. The mathematical treatment presented in the current publication provides a rigorous solution to a more general approach in which both parameters, H and $\omega^2 t$ products, can be varied.

Spreading of the boundary can be the consequence of polydispersity or it can be due to diffusion of solute molecules under the influence of the concentration gradient originated during centrifugation. Discrimination between these two effects in the current methodology follows the same line of approach used in conventional centrifugation techniques. Attempts to estimate the diffusion coefficient would be, however, more laborious, though not impossible.

Theoretical

Successive Aliquot Extractions. When ordinary centrifuge tubes are used as sedimentation cells, provided that their inside diameter does not exceed 5 mm to avoid excessive perturbation against the walls as demonstrated in Pita and Müller (1972), it is possible to collect several fractions along the tube length after centrifugation is completed. When analyzed for solute concentration these fractions provide knowledge of a concentration *vs.* radial coordinate curve (Figure 1B). The concentrations found are mean concentration values at intervals Δx, approaching the point values C_x when Δx becomes very small. This curve can be used in the same way as a concentration diagram provided by standard analytical ultracentrifuges. By differentiation a schlieren curve, dc/dx, is found and, from it, the distribution functions $g(s)$ and $G(s)$ can be calculated. The transformation of dc/dx into the $g(s)$ function should be done according to the following equation

$$g(s) = \frac{\omega^2 t}{C_0}\frac{dc}{dx}\frac{x^2}{x_m} \qquad (1)$$

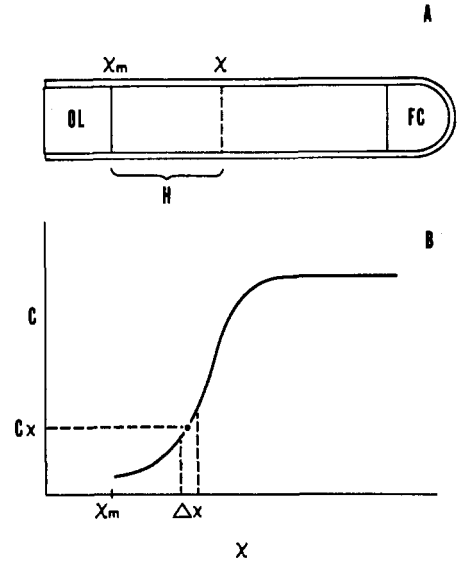

FIGURE 1: Sedimentation capillary cell and representative concentration diagram. (A) OL = oil layer to prevent evaporation; x_m = meniscus radial coordinate from rotor center; x = radial coordinate of variable partition plane; H = length of "supernatant" solution partitioned or extracted from the tube; FC = fluorocarbon layer. (B) The experimental concentrations found by the method of successive aliquot extractions are a mean concentration value at the interval Δx, approaching the point value, c_x, if Δx is very small.

where x_m is the meniscus radial coordinate, ω is the angular speed, t is the time, C_0 is the initial concentration, and x is the point coordinate. This expression contains the term (x^2/x_m) instead of the usual (x^3/x_m^2). This is due to the fact that a linear and not a quadratic dilution law has been adopted, in practice, for a cell of constant cross section (Pita and Müller, 1972).

Integral Supernatant Concentrations. When working with capillary microcells, several of which are simultaneously centrifuged and where successive extractions along the tube length are not possible, the method of cutting a whole section of solution of length H from the meniscus to a given plane at x has to be used (Figure 1A). Obviously, after centrifugation and homogenization of this centripetal fraction, a final concentration (C_F) is obtained, corresponding to the integral

$$C_F = \int_{x_m}^{x} c\,dx \Big/ \int_{x_m}^{x} dx = \frac{1}{x - x_m}\int_{x_m}^{x} c\,dx \qquad (2A)$$

Since $x - x_m = H$ and $dx = dH$, the above expression can be written as

$$C_F H = \int_0^H c\,dH \qquad (2B)$$

Differentiation with respect to H leads to

$$\frac{d}{dH}[C_F H] = c \qquad (3)$$

Equation 3 indicates that if a plot of $C_F H$ *vs.* H is constructed with the experimental C_F values obtained for each H, the derivative of this plot gives the point concentration value c as a function of H. Figure 2A shows the appearance of such a plot for a hypothetical gaussian distribution of coefficients and the solid line in Figure 2B indicates the corresponding

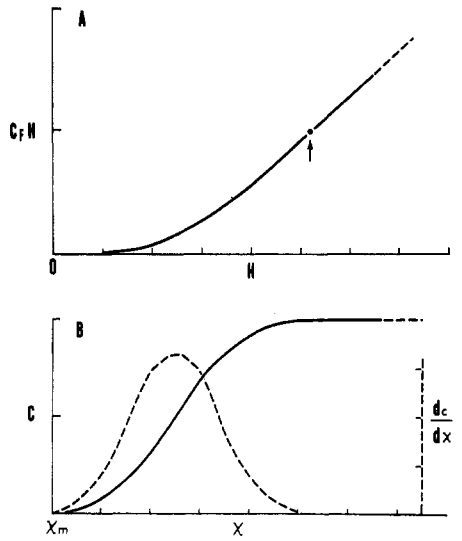

FIGURE 2: Ideal concentration plots for a gaussian distribution of coefficients. (A) Integral concentration curve plotted as $C_F H$ product *vs.* H. The straight line above the arrow corresponds to the plateau region. (B) (—) point concentration curve obtained as the derivative of the upper curve. Since x and H are easily interchangeable the horizontal scale has been adjusted in terms of x so that $x = x_m$ for $H = 0$; (- - -) point concentration gradient, dc/dx, obtained by differentiating the previous curve with respect to x.

derivative curve. From the latter curve the boundary gradient curve dc/dx can be obtained through a second process of differentiation (dashed line in Figure 2B). This schlieren-type curve is used in connection with eq 1 and the distribution function is obtained. This mathematical procedure can be summarized by combining eq 1 and 3 into a single expression

$$g(s) = \omega^2 t \frac{x^2}{x_m} \frac{\partial}{\partial x}\left[\frac{\partial}{\partial H}\left(\frac{C_F}{C_0} H\right)\right]_{\omega^2 t} \quad (4)$$

where the subscript $(\omega^2 t)$ indicates that the data have to be obtained by selecting a constant value for this parameter.

It should be noted that the point marked with an arrow in Figure 2A denotes a discontinuity in the plot since it separates the boundary gradient region (left) from the plateau region (right), the latter being, in fact, a straight line and not a curve. Correspondingly, the first and second derivatives are, respectively, constant and zero as evidenced by the curves in Figure 2B for the plateau region.

This approach assumes that the spreading of the boundary can be encompassed within the limits of the capillary cell length. In practice there is always a minimum length, H_m, that can be reliably processed with the analytical assay at hand and a maximum length, H_M, that can be partitioned off the tube without getting too close to its bottom. Let s_m and s_M denote, respectively, the minimum and maximum coefficient values in the distribution and let $(\omega^2 t)$ be so chosen that the boundary of s_m traverses exactly the minimum length H_m. Then, since the coefficients are grossly proportional to their boundary locations we can write, approximately

$$H_M/H_m = s_M/s_m \equiv R \quad (5)$$

Now, when the ratio R is 5, or more, it is usually impossible to study the whole distribution within a single centrifugation setting. Then the method of changing the products $\omega^2 t$ has to be applied.

Stepwise Procedure with Several $\omega^2 t$ Settings. The $C_F H$ plot needed to apply eq 4 cannot be constructed with data coming from experimental runs having different $\omega^2 t$ settings in the centrifuge. If the distribution of coefficients cannot be completely studied within a single $\omega^2 t$ setting, as mentioned in the preceding section, then it is possible to break down the study into several ranges of coefficients. To analyze each range the H parameter can be varied while keeping constant the product $\omega^2 t$ at a selected value. Then, the transformation factor $\omega^2 t (x^2/x_m)$ included in eq 4 will allow the combination of the different portions of the $g(s)$ curve found into a continuous and complete distribution.

In some interesting but difficult cases the available biological samples are extremely small and cannot be stored for pooling purposes but can be periodically and reproducibly collected. In these cases it might not be possible to change the H-length values as needed to cover even a limited portion of the distribution range. The situation is similar to that encountered when studying polydisperse distributions with a fixed partition cell (H = constant), in which case, the only variable available is the parameter $\omega^2 t$. To this effect, Watanabe *et al.* (1954) have used the following approximate formula to predict the C_F/C_0 ratios in a standard sectorial cell

$$C_F/C_0 \approx \frac{1}{Z}\int_0^Z (Z - s) g(s) ds \quad (6)$$

Here $g(s)$ is the differential distribution function to be found, s is the sedimentation coefficient of a given species in the distribution with $s \leqslant Z$, and Z is, in turn, the sedimentation coefficient of that species (real or hypothetical) whose boundary should have just reached the partition plane at the end of the run. Obviously Z is related to $\omega^2 t$ and H (or x), by the classical formula

$$Z = \frac{1}{\omega^2 t} \ln\left(\frac{x_m + H}{x_m}\right) \quad (7A)$$

$$x = x_m e^{Z\tau} \quad (7B)$$

where $x = x_m + H$ and the symbol τ has been introduced for $\omega^2 t$.

As a basis to evaluate the approximation implied in eq 6, especially for cylindrical capillary cells, the following analysis has been considered necessary. A rigorous calculation of C_F/C_0 as a function of Z, H, x_m, and τ is as follows. If no diffusion is present any species with coefficient s will locate its boundary at

$$x_s = x_m e^{s\tau} \quad (8)$$

The contribution ΔC_F to the total final concentration, after the cell is partitioned and homogenized, due to this single species, will be, by eq 5 of Pita and Müller (1972)

$$\Delta C_F = \Delta C_0 \left(\frac{x - x_s}{x - x_m}\right)\left(\frac{x_m}{x_s}\right) \quad (9)$$

where ΔC_0 is that fraction of the total initial concentration, C_0, corresponding to this particular species, namely

$$\Delta C_0 = C_0 g(s) \Delta s \quad (10)$$

(Δs being a small interval of coefficients whose midpoint is close to that of the species in question). Substituting eq 10 in eq 9 and adding for all the species in the supernatant, *i.e.*, those with $0 \leqslant s \leqslant Z$, we obtain

$$\frac{C_F}{C_0} = \int_0^z \frac{x_m}{x_s}\left(\frac{x - x_s}{x - x_m}\right)g(s)ds \qquad (11)$$

Using eq 7B and 8, and recalling that $x - x_m = H$, eq 11 can be rewritten as

$$\frac{C_F}{C_0} = \int_0^z \frac{1}{e^{s\tau}}\left(\frac{x_m e^{z\tau} - x_m e^{s\tau}}{H}\right)g(s)ds = \frac{x_m}{H}\int_0^z (e^{(z-s)\tau} - 1)g(s)ds \qquad (12)$$

In order to obtain $g(s)$ it is now necessary to differentiate eq 12 with respect to Z, but since H is functionally related to Z through eq 7A it is preferable to multiply the ratio C_F/C_0 by the parameter H/x_m and to consider the new function

$$\frac{C_F}{C_0}\frac{H}{x_m} = e^{z\tau}\int_0^z e^{-s\tau}g(s)ds - \int_0^z g(s)ds \qquad (13)$$

where the integrals have been separated. Assuming now a constant τ and differentiating[1]

$$\frac{d}{dZ}\left[\frac{C_F H}{C_0 x_m}\right] = e^{z\tau}e^{-z\tau}g(Z) + \tau e^{z\tau}\int_0^z e^{-s\tau}g(s)ds - g(Z) = \tau e^{z\tau}\int_0^z e^{-s\tau}g(s)ds$$

Differentiating again

$$\frac{d^2}{dZ^2}\left[\frac{C_F H}{C_0 x_m}\right] = \tau e^{z\tau}e^{-z\tau}g(Z) + \tau^2 e^{z\tau}\int_0^z e^{-s\tau}g(s)ds = \tau g(Z) + \tau\frac{d}{dZ}\left[\frac{C_F H}{C_0 x_m}\right]$$

Solving for $g(Z)$

$$g(Z) = \frac{1}{\tau}\frac{d^2}{dZ^2}\left[\frac{C_F H}{C_0 x_m}\right] - \frac{d}{dZ}\left[\frac{C_F H}{C_0 x_m}\right] \qquad (14)$$

indicating that an experimental plot of $C_F H/C_0 x_m$ *vs.* Z and its two derivatives can provide the function $g(s)$ for each Z used. The result, however, is dependent upon a constant τ (or $\omega^2 t$) and this precludes the use of eq 14 with experimental points in which the products $\omega^2 t$ are not the same. Equation 12, therefore, in spite of its rigorous character defeats the purpose it was intended for. If certain approximations are made, however, then variations in $\omega^2 t$ can be ignored. For instance in eq 12 we can approximate $e^{(z-s)\tau} - 1 \approx (z - s)\tau$ and from eq 7A $z \approx H/\omega^2 t x_m$ or $x_m/H \approx 1/Z\omega^2 t$. Substituting these results in eq 12 we have

$$\frac{C_F}{C_0} \approx \frac{1}{Z\omega^2 t}\int_0^z (Z - s)\omega^2 t g(s)ds = \frac{1}{Z}\int_0^z (Z - s)g(s)ds$$

which is exactly eq 6 as used by Watanabe *et al.* (1954) and which is independent of τ. In this simplified form all the variables are contained within the single parameter Z and differentiation of the functional product $Z(C_F/C_0)$ two times with respect to Z readily yields $g(Z)$. Thus, multiplying by Z

$$Z\left(\frac{C_F}{C_0}\right) = Z\int_0^z g(s)ds - \int_0^z sg(s)ds \qquad (15)$$

Differentiating[1]

$$\frac{d}{dZ}\left[Z\frac{C_F}{C_0}\right] = Zg(Z) + \int_0^z g(s)ds - Zg(Z) = \int_0^z g(s)ds \qquad (16)$$

and

$$\frac{d^2}{dZ^2}\left[Z\frac{C_F}{C_0}\right] = g(Z) \qquad (17)$$

Therefore, an experimental plot of $Z(C_F/C_0)$ *vs.* Z and its second derivative will give $g(s)$ for any Z value used, regardless of the $\omega^2 t$, H, or x_m values used.

Plateau Region. In the case of successive aliquot extractions the plateau region will evidently be noticed by the constancy of the concentrations found in that region. For the other methods of studying polydispersity it should be noticed, however, that eq 6 and 12 predict the C_F/C_0 values only when the Z corresponds to a partition plane lying in the boundary gradient region. The function $g(s)$ is zero throughout the plateau region and both equations become meaningless there. However, in the actual laboratory measurement of an unknown $g(s)$ distribution it is likely that some of the partition marks used will fall in the plateau region and corresponding C_F/C_0 values will be obtained. These values can be theoretically accounted for by a linear combination of the homogenized final concentration coming from the complete boundary region plus that portion of the plateau being included. The former concentration is given by eq 12 using for Z the maximum sedimentation value in the distribution, whereas the plateau (point) concentration, C_p, is given by an equation similar to eq 12 but considering only the linear dilution law ($e^{-s\omega^2 t}$) as affecting the concentration of every species in the plateau. Adding this effect for all species

$$C_p/C_0 = \int e^{-s\omega^2 t}g(s)ds \qquad (18)$$

where the integration should cover the whole distribution range. Combining this concentration with that of the homogenized total boundary region, $(C_F/C_0)_B$, extended from the meniscus to the location of the fastest component, say, at H_M, the ratio C_F/C_0 for a total column of length H reaching the plateau region ($H > H_M$) is

$$(C_F/C_0)_{plat} = \frac{H_M(C_F/C_0)_B + (H - H_M)C_p/C_0}{H} = \frac{H_M[(C_F/C_0)_B - C_p/C_0]}{H} + C_p/C_0 \qquad (19)$$

The term between brackets is a constant, K, for a given $\omega^2 t$ and x_m setting, so, after multiplication by H, the above equation becomes

$$H\left(\frac{C_F}{C_0}\right)_{plat} = K + \frac{C_p}{C_0}H \qquad (20)$$

[1] Throughout this derivation the mathematical relationship $(d/dy)\cdot[\int_0^y f(x)dx] = f(y)$ has been used.

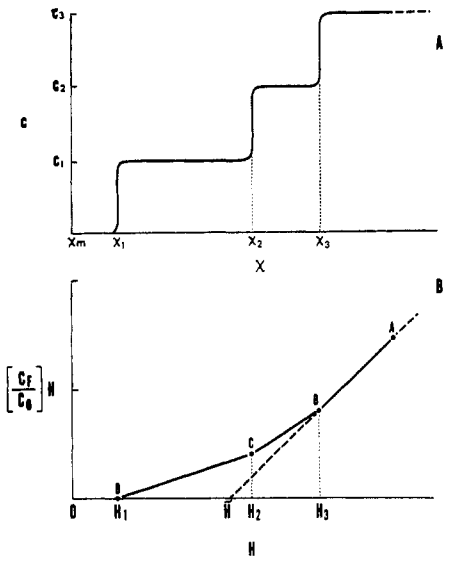

FIGURE 3: Theoretical concentration plots for a three-component system. (A) Point concentration curve showing the plateau concentration levels C_1, C_2, and C_3 (still uncorrected for radial dilution). x_1, x_2, and x_3 are the corresponding boundary locations. (B) Integral concentration plot. The product $C_F H$ has been divided by C_0 so the slope of the upper right-hand segment is almost unity (same scale unit in both axis). H_1, H_2 and H_3 show the boundary locations corresponding to x_1, x_2, and x_3 in the upper curve. The horizontal scale was adjusted so that $x = x_m$ for $H = 0$. $\bar{H}$ indicates the ideal boundary location of the "centrifugal" average sedimentation coefficient ($\bar{s}_c$).

demonstrating that the $(C_F/C_0)H$ group or, for that matter, the $C_F H$ product, is a linear function of H throughout the plateau region, confirming what was said above in connection with Figure 2A.

The advantage of plotting $(C_F/C_0)H$ *vs.* H instead of $C_F H$ is that the slope of the plot in the former case, and not the latter, is C_p/C_0. This ratio is usually very close to unity and makes it possible to recognize the plateau region by its 45° inclination even with only two experimental points on it. Of course when the radial dilution effect becomes prominent C_p/C_0 is decreased and the slope of the graph is significantly flattened.

Paucidisperse Systems. The preceding theory for the plateau region leads smoothly into the study of paucidisperse systems. These could be considered as consisting, essentially, of several plateau regions, each one containing one more species than the other till a common plateau region is reached in which all species are present. Since the plot of a plateau region is a straight line it is easy to deduce that a paucidisperse system will also yield a plot consisting of several straight segments meeting at sharp angles. The number of such segments is equal to the number of components present in the mixture.

For simplicity, a three-component system will be considered with coefficients s_1, s_2, and s_3 in increasing order of magnitude and with respective initial concentrations C_{0_1}, C_{0_2}, and C_{0_3} (so that $C_{0_1} + C_{0_2} + C_{0_3} = C_0$).

If the system is studied by the method of successive aliquot extractions then a concentration *vs.* x diagram, like the one shown in Figure 3A, will be obtained. The sedimentation coefficients can be calculated by substituting the boundary locations x_1, x_2, and x_3 in the classical formula

$$s = \frac{1}{\omega^2 t} \ln (x/x_m) \qquad (21)$$

For calculating the initial compositions the differences between C_3, C_2, and C_1 (shown in the ordinate axis) can be used, provided they are corrected fo the radial dilution effect. In other words:

$$\begin{aligned} C_{0_1} &= C_1 e^{s_1\omega^2 t} \\ C_{0_2} &= (C_2 - C_1)e^{s_2\omega^2 t} \\ C_{0_3} &= (C_3 - C_2)e^{s_3\omega^2 t} \end{aligned} \qquad (22)$$

On the other hand, if integral supernatant concentrations have to be used and the experimental data can be obtained at least in a certain range of H by keeping $\omega^2 t$ and x_m constant, then the plot of $(C_F/C_0)H$ *vs.* H will look as illustrated in Figure 3B. To establish such a plot it would be necessary to have at least three experimental points in each chord, to assure their rectilinear character. Granted this to be the case, the coefficients can be calculated by using the parameters H_1, H_2, and H_3 (shown on the abscissa axis). These parameters indicate the coordinates where the boundaries are located. Equation 21 is then applied, remembering that $x_1 = H_1 + x_m$; $x_2 = H_2 + x_m$; etc. To calculate the initial compositions the result expressed by eq 3 ought to be recalled. This equation expresses that the slope of each rectilinear segment, in the $C_F H$ or the $(C_F/C_0)H$ plot, gives the point concentration values along those segments. Hence, denoting the different slopes by the symbol m, the following relationships can be written: $m_{CD} = C_1/C_0$, $m_{BC} = C_2/C_0$, and $m_{AB} = C_3/C_0$. These concentrations are identical with those of Figure 3A except that they have been divided by the total initial concentration. As in the previous case they can be corrected for the radial dilution effects ($e^{s\omega^2 t}$), and the ratios C_{0_1}/C_0, C_{0_2}/C_0, and C_{0_3}/C_0 are obtained using eq 22.

Finally, if points obtained with different $\omega^2 t$ settings have to be used for studying the system then the ZC_F/C_0 *vs.* Z plot can be utilized. This plot has the same appearance and essential features as the previous one except that now the first derivative or slope of each segment gives, directly, the integral distribution function, $G(s)$, as implied by eq 16. This equation was derived for a continuous or polydisperse system but it can be easily adapted to study a paucidisperse one. Suppose, for example, that Z_1, Z_2, and Z_3 are now the points at which the polygonal segments meet. Then the integral function $G(s)$ or slope of each segment will change abruptly at each meeting point, the difference in slope, or $G(s)$, being, therefore, the amount of material attributable to that particular Z value where the change occurred.

The two plots $(C_F/C_0)H$ *vs.* H and $(C_F/C_0)Z$ *vs.* Z are also comparable in the following respect. If the segment representing the common plateau region (AB in Figure 3B, with slope close to unity) is produced to intersect the horizontal axis, the parameter $\bar{H}$ indicates the ideal boundary location of a hypothetical monocomponent system that could replace the paucidisperse system in the ultracentrifuge and behave in exactly the same way as far as transport measurements in the plateau region are concerned. The same thing holds true for the ZC_F/C_0 plot, giving an average $\bar{Z}$ value on the horizontal axis which, although differing conceptually from the weight average coefficient of the mixture, is, however, very close to it (see Discussion).

Combined Paucidispersity, Polydispersity, and Diffusion Effects. In practice there is seldom an opportunity to obtain an ideal polygonal plot like the ones referred to in the previous section. The frequent case is that paucidispersity will be partially obscured by more or less extended curvatures at

the meeting points of the polygonal segments. This "curving" effect can be due to intrinsic polydispersity within the different components or it can be due to diffusion effects at each interboundary region. If the blurring is not too severe it might be possible to prolong the straight portions of each segment so that their meeting points can be discovered. If not, the process of finding the derivatives should reveal the different peaks even if there is partial overlapping as so frequently occurs in ultracentrifugal studies.

Another problem is that of distinguishing between polydispersity and diffusion effects. This can be done by comparing two runs in which the times and angular speeds are different but the products $\omega^2 t$ are the same. If the plots remain identical then all curvatures are strictly due to polydispersity but if variations are detected then diffusion forces (which depend on the square root of the time) are evidently operative. Combined polydispersity and diffusion effects in which the latter factor is significant can be corrected by extrapolating the apparent $g(s)$ functions obtained to an infinite time of centrifugation as regularly done with the analytical ultracentrifuge (Schachman, 1959). In the present methodology this procedure would require several runs at increasing times, each one being equivalent to a photograph of the analytical ultracentrifuge. For the special case of a monocomponent system showing spreading of the boundary by diffusion alone it might be possible to estimate the diffusion coefficient itself.

Experimental Section

Materials and Methods. All chemicals used were analytical grade from Mallinckrodt Chemical Works. The human serum albumin was obtained from Calbiochem, and the proteoglycan subunit and proteoglycan complex were kind gifts from Dr. Lawrence Rosenberg, New York University, and Dr. Stanley Sajdera, State University of New York. The centrifuge used was a Model L Beckman preparative ultracentrifuge with an SW 50.1 swinging bucket rotor.

The spectrophotometer was a Zeiss PMQII model with microcells MS5 Zeiss and the microcuvet of 3.1-cm light path and 8.4-μl capacity described in Howell *et al.* (1966). Capillary cells were the same as previously described (Pita and Müller, 1972). Cellulose tubes, 5 mm in diameter (Beckman 305528), were also used for larger volumes. These were used with their commercially available adapters (Beckman 305527) except that screw aluminum caps were made to hold the tubes from the top and avoid excessive pressure against the walls which would render it impossible to remove the tubes without disturbing the sedimentation boundaries. A small water volume (0.15 ml) was added between the tubes and the adapter wall to completely cancel external pressures during centrifugation. Proteins were determined by the Lowry *et al.* (1951) method. Hexuronic acid determinations were conducted with the Bitter and Muir (1962) modification of the carbazole method of Dische (1947) with D-glucuronic acid (Sigma) as standard.

Experimental Procedure. Selection of the method for studying polydispersity or paucidispersity depends very much upon the volume and concentration of the sample and the distribution range of the biological species involved in the study. Successive aliquot extractions can be done with a regular bottom piercing device like the ones used for density gradient centrifugation. A layer of fluorocarbon, FC-43 (Spinco-Beckman), can be used as in usual ultracentrifugal practice. Since solute molecules accumulate at the fluorocarbon–water interface during centrifugation it is recommendable to discard the first few drops together with the fluorocarbon layer in order to avoid contaminating the remaining aliquots.

Integral supernatant concentrations in capillary cells or in cellulose tubes are done exactly as described by Pita and Müller (1972). When very small volumes of diluted solutions were ultracentrifuged in the capillary microcells the solute concentrations in the centripetal fractions were determined spectrophotometrically by using the cuvet described in Howell *et al.* (1966). Centrifugation time and angular speed are measured also as described by Pita and Müller (1972).

Information about the extent of the plateau region is readily obtained with the current methodology. Two points in the $(C_F/C_0)H$ plot, inclined at slope 1, or very close to it, are sufficient to locate the plateau region and to calculate the average sedimentation coefficient of the system. Then the centrifugal parameters (mainly H and $\omega^2 t$) can be chosen to obtain points which gradually depart from the plateau region and fall more within the boundary region. Additional runs, necessary for checking the influence of diffusion, need not be repeated over the entire range of points analyzed.

When using the approximate method of eq 17 the possibility exists that temperature levels vary from run to run (since the speeds are different for each one). To make comparisons possible it is necessary, then, to correct every Z value used to standard conditions (usually 20°) before making the $Z(C_F/C_0)$ plot. Once this is done the $g(s)$ values obtained are automatically corrected to standard conditions. On the other hand, if eq 4 is used at a temperature other than 20° the $g(s)$ curve obtained can be corrected *a posteriori* to standard conditions as in usual ultracentrifugal practice (Schumaker and Schachman, 1957). The same correction applies to this equation when used at different $\omega^2 t$ and temperatures for separate ranges of the distribution.

Results and Calculations

Biological standards were chosen to illustrate some of the cases considered in the theoretical section of this paper.

Human Serum Albumin. At a level of 1.1% concentration in 0.2 M phosphate buffer (pH 6.0) this protein served as an example of a monodisperse system affected only by diffusion spreading of the boundary. The sample was studied by the method of integral supernatant concentrations in 36 capillary cells of 1.2 mm inside diameter and 12 mm length. The H lengths used varied from 2 to 8 mm. Figure 4 shows the $(C_F/C_0)H$ plot obtained after centrifugation of the cells at 44,000 rpm for 46.3 min ($\omega^2 t = 5.9 \times 10^{10}$ sec^{-1}). All menisci were placed at 8.03 cm from rotor center. Each point was run six times and at least four of them, C, D, E, and F, laid in a straight line of slope 1, evidencing the plateau region. Sedimentation coefficients calculated from these points by the method of Pita and Müller (1972) gave an average s value of 4.4 S ± 3% which is to be compared with the value of 4.3 S given by Pedersen's regression line at a comparable concentration as quoted by Charlwood (1952). This close agreement indicates the presence of almost a pure system, ruling out significant contribution of polydisperse or paucidisperse components. Consequently the curvature indicated by points A, B, and C in the graph must be entirely due to diffusion effects. This fact allowed estimation of the diffusion coefficient by means of the length L_D as shown in Figure 4. The point H_b in the abscissa axis corresponds to the ideal boundary location of the solute if no diffusion had occurred. Hence, using the simple theory of diffusion in the ultracentrifuge of Svedberg and Pedersen (1940), L_D represents the variable

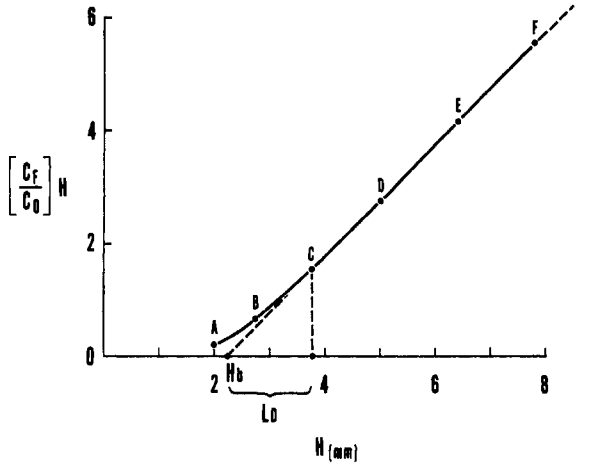

FIGURE 4: Integral concentration plot obtained for a sample of human serum albumin. H_b is the ideal boundary location and $L_d = 4(Dt)^{1/2}$. The point of departure at C was also found by replotting the C_F/C_0 data *vs.* $1/H$ (see Pita and Müller, 1972). C, D, E, and F laid in the plateau region (slope one).

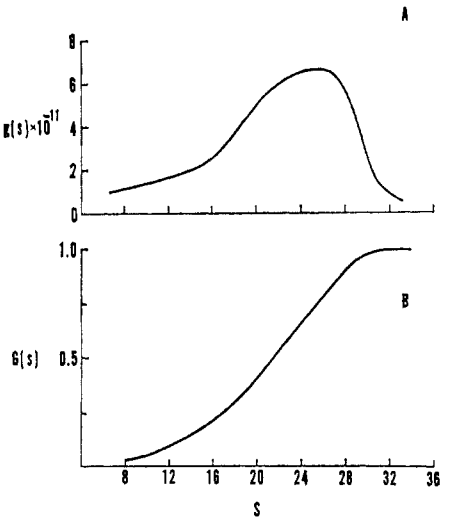

FIGURE 5: Experimental distribution functions for the proteoglycan subunit. (A) Differential distribution function $g(s)$ obtained from the experimental dc/dx curve (not shown) and applying eq 1. (B) Integral distribution $G(s)$ obtained by integration of the upper curve. The horizontal scale is in Svedberg units.

$z = y(4Dt)^{1/2}$ where $y = 2$ (practical upper limit) (Schack, 1965). Since L_D is 1.56 mm and the time was 46.3 min the diffusion coefficient is

$$D = \frac{1.56^2 \times 10^{-2}}{16 \times 46.3 \times 60} = 5.6 \times 10^{-7}\ \text{cm}^2\ \text{sec}^{-1}$$

This result is somewhat lower than the mean value usually offered in the literature (Charlwood, 1952), which is 6.1×10^{-7} Ficks at a similar concentration. This discrepancy will be considered later in the Discussion.

Proteoglycan Subunit. A 0.08% solution of proteoglycan subunit in 0.15 M KCl was investigated by the method of integral supernatant concentrations (a) in the same capillary microcells mentioned above and eight of these cells, with H values from 2.0 to 8.0 mm, were ultracentrifuged simultaneously (b) in 5 mm i.d. cellulose tubes. In this case centripetal fractions were collected, at the end of the run, with a syringe from above the tubes, the length H being a function of the volume of solution removed. All the data were obtained with the same $\omega^2 t = 8.72 \times 10^{10}$ sec^{-1} and with a correspondingly constant x_m. Results obtained using the technique at ultramicro and micro levels were used to plot the corresponding $(C_F/C_0)H$ *vs.* H curves. From these plots and by two successive differentiation processes, curves of dc/dx *vs.* x were obtained by subdividing the boundary region into 15 equally spaced intervals. Equation 1 was applied and the results are shown in Figure 5A. The integral distribution function $G(s)$ (Figure 5B) was also obtained by numerical integration of Figure 5A.

The distribution appears to be asymmetrically extended from below 8 S to about 34 S with a peak at 25.5 S. The average value, however, calculated from the point at $G(s) = 0.5$ was only 21.5 S, significantly different from the peak value.

Another proteoglycan subunit sample was used to verify that the curvature of the plots was entirely due to polydispersity and was not affected by diffusion effects. Three runs were made: two with the same $\omega^2 t$ products but different times and speeds and a third one with an altogether different $\omega^2 t$ product. On account of this difference in $\omega^2 t$ the concentration data obtained were plotted by the Z methodology as shown in Figure 6 so that superimposition of the curves could be expected. The points represented by full and open circles were run at the same $\omega^2 t$ ($=9.97 \times 10^{10}$ sec^{-1}) but the total time of the latter was more than twice that of the former points as indicated in the legend of the figure. Triangular points correspond to a run with $\omega^2 t = 6.57 \times 10^{10}$ sec^{-1}. Coincidence of all the plots evidenced the virtual absence of diffusion perturbations.

Proteoglycan Complex. The combined effects of polydispersity and paucidispersity were studied in a 0.04% solution of proteoglycan complex by the method of successive aliquot extractions. Ultracentrifugation was conducted at 35,210 rpm for 52.8 min ($\omega^2 t = 4.31 \times 10^{10}$ sec^{-1}). The first five of a total of 25 drops, collected by piercing the bottom of the cellulose tube after centrifugation, were discarded and the rest was analyzed for hexuronic acid concentration. Each drop represented 1-mm distance along the tube length. A concentration *vs.* x curve was made with the data as shown in Figure 7A. The two broad sigmoid curves separated by a short but definite straight portion around $x = 8.2$ cm clearly indicated the existence of two main components as expected for this kind of preparation (Franek and Dunstone, 1967; Hascall and Sajdera, 1969; Rosenberg *et al.*, 1970). Transformation of the curve into the distribution function by eq 1 was done and the result is shown in Figure 7B. The first peak in the distribution, with a maximum at 21.5 S, is in agreement with the proteoglycan subunit shown in Figure 5A, confirming its nature as a basic component of the complex. On the other hand, the second peak or fast sedimenting component showed a maximum at 55 S. Integration of the areas under the peaks gave relative proportions of 54 and 46% for the slow and fast components, respectively.

Error Considerations. Analytical deviations in determining the loading concentration, C_0, or the final concentrations after centrifugation, can influence, significantly, the value of the distribution function obtained. Since this function is obtained, in general, as a second derivative curve of the experimental data, the errors can be as large as four times the imprecision in the analyses. Highly precise assays are, therefore, recommended and the use of statistically significant averages is needed. The advantageous possibility of centrifuging simultaneously several cellulose tubes in a rotor with six holders

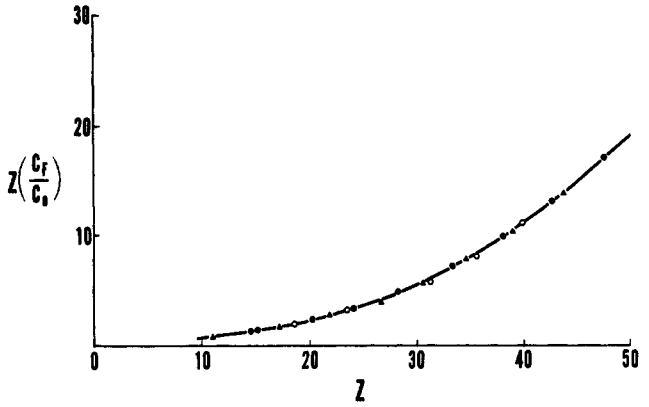

FIGURE 6: Experimental $Z(C_F/C_0)$ plot for three different runs of a proteoglycan subunit sample. The centrifugation times were: (●) 52 min; (▲) 70 min; (○) 120 min. The $\omega^2 t$ values were: 6.57×10^{10} (▲) and 9.97×10^{10} (○, ●).

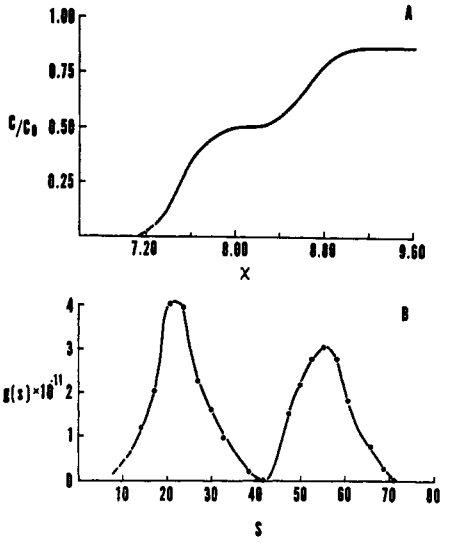

FIGURE 7: Ultracentrifugal study of the proteoglycan complex by successive aliquot extractions.(A) Experimental point concentration curve. (B) Differential distribution function obtained from the upper curve by means of eq 1 (horizontal scale in Svedberg units).

or as many as eight capillaries in each holder as the one described in publication (Pita and Müller, 1972) facilitates the attainment of the necessary number of experimental values for each H used.

To estimate the approximation involved in the simplified mathematical treatment of eq 6 and 17 a hypothetical trigonometric distribution of coefficients has been numerically investigated. This function closely resembles a gaussian distribution (see Figure 8) and is given by

$$g(s) = \frac{2}{s_M} \sin^2 \theta \qquad (23)$$

where s_M represents the maximum coefficient in the distribution and θ is defined as $\theta \equiv \pi s/s_M$. The coefficients s cover the interval from 0 to s_M with a peak at $S_M/2$ (where $\sin \theta$ is a maximum). Hence, the interval for θ should be 0–π, outside of which it is meaningless. If s_M is given the value 50×10^{-13} sec, the distribution extends, symmetrically, from 0 to 50 S with a peak at $\bar{s} = 25$ S (weight average sedimentation coefficient of the mixture). In terms of $\bar{s}$, eq 23 can be rewritten as shown in the Appendix (eq II). Equation III, also in the Appendix, gives the integral distribution function $G(s) = \int g(s)ds$ and eq IV is the result of integrating eq 12 to predict the exact C_F/C_0 expected values. Equation V predicts the same ratios but by the approximate method of eq 6.

Table I is a comparative presentation of the results obtained for the selected Z values shown in the first column. The second and third columns give the predicted C_F/C_0 ratios by the exact (eq IV) and approximate methods (eq V), respectively. It is seen that the approximation is generally by excess, of the order of 0.5–3%, with an average 2.1% error. The next column shows the exact values of the distribution function as obtained directly from eq 23 and the last column gives the same function as calculated by eq 17. The second derivative necessary to apply this equation was obtained as in an experimental situation, using intervals ΔZ of 5 Svedberg units above and below the selected Z value. The results shown in this column are all by defect with an average error of 4%. Consequently, when analytical deviations are not better than 1% the use of eq 17 is justified.

TABLE I: Comparison of Exact and Approximate $g(s)$ Calculations for a Trigonometric Distribution of Coefficients.[a]

Z[b]	C_F/C_0	C_F/C_0	$g(s)$	$g(Z)_\Delta$
50	0.4849	0.5000	0.000	
45	0.4317	0.4446	0.382	0.409
40	0.3677	0.3781	1.382	1.330
35	0.2948	0.3026	2.618	2.489
30	0.2185	0.2236	3.618	3.414
25	0.1457	0.1487	4.000	3.795
20	0.0841	0.0854	3.618	3.481
15	0.0393	0.0395	2.618	2.526
10	0.0129	0.0125	1.382	1.362
5	0.0017	0.0016	0.382	0.446
0	0.0000	0.0000	0.000	

[a] All the figures given for the g function in this table have been multiplied by 10^{-11}. [b] In Svedberg units.

Discussion

Restricted diffusion against the meniscus in the early stages of centrifugation is a factor whose influence is dif-

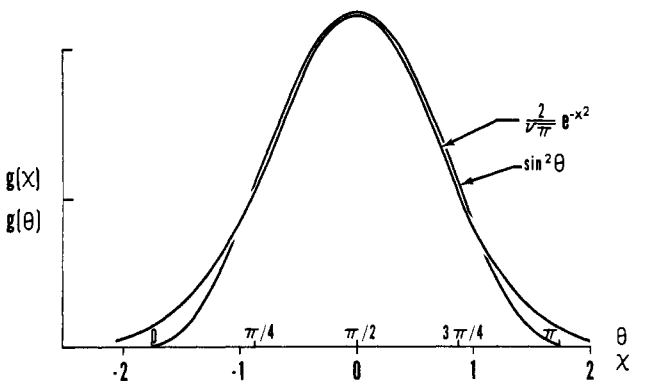

FIGURE 8: Comparison of the error function $(2/\sqrt{\pi})e^{-z^2}$ with the trigonometric $\sin^2 \theta$ function. The deviation at the foot of the curves is not too relevant since actual sedimentation coefficient distribution might also depart from a strictly gaussian distribution.

ficult to assess in transport considerations. With conventional optical techniques it is usually sufficient to delay the taking of the first photographs so that initial distortions of the boundary become practically unimportant. The results obtained for the diffusion coefficient of human serum albumin in this paper, however, seem to indicate a possible permanent distortion in diffusion transport, explaining the somewhat lower value obtained in estimating the diffusion coefficient of this protein. Calculation of diffusion coefficients is, however, only a collateral application of the current methodology and nonessential to it.

Typical polydispersity problems, like that of the proteoglycan subunit sample given in Figure 5, demonstrated reasonable experimental agreement with already published data. For instance, Hascall and Sajdera (1970) obtained for a similar proteoglycan subunit preparation, studied at this level of concentration with a conventional analytic ultracentrifuge, a distribution ranging from about 7 to 34 S, with an average value of 20 S instead of the 21.5 S found in this report. Their distribution was also "skewed" toward the higher values of coefficients.

The results obtained for the proteoglycan complex preparation are also in good agreement with the data published by several investigators (Franek and Dunstone, 1967; Hascall and Sajdera, 1969; Rosenberg *et al.*, 1970). The typical bimodal behavior of this complex includes a fast sedimenting mode with an average sedimentation coefficient of about 60 S and a slow sedimenting component similar to the proteoglycan subunit with respect to its average sedimentation value and its polydisperse distribution.

The numerical values used in the trigonometric example of eq 23 were chosen so that radial dilution effects had a moderate intensity upon the average sedimenting species ($\bar{s}$ = 25 S), producing a decrease to about 93% of its initial concentration. It should be pointed out that the approximation implied in eq 6 holds better for the kind of cells used in this investigation than it would in standard sectorial cells. For instance, in Table I, $C_F/C_0 = 0.4849$ for $Z = 50$, but for a standard sectorial cell the expected value would have been 0.4677 which is farther removed from the 0.5000 value predicted by eq 6.

The "centrifugal average" value, $\bar{s}_c$, referred to in the theory of paucidisperse systems, corresponds to the coefficient of a hypothetical substance whose behavior in the ultracentrifuge would exactly duplicate the behavior of the actual system, as far as mass transport in the plateau region is concerned. This average, $\bar{s}_c$, obeys the relationship

$$\exp(-\bar{s}_c\omega^2 t) = \sum f_i \exp(-s_i\omega^2 t)$$

where f_i is the weight fraction, C_{0i}/C_0, of the ith component and s_i is the corresponding sedimentation coefficient. This is to be compared with the usual definition of $\bar{s}_w$ (weight average sedimentation coefficient), $\bar{s}_w = \Sigma f_i s_i$, the latter being equivalent to the former only when the exponential functions can be approximated. For most practical purposes both concepts can be considered equivalent.

Extrapolation to infinite dilution to obtain the $g(s)$ function at zero concentration (symbolically $g(s_0)$) is usually avoided by working at high dilutions. In general, transport methodology allows determination of sedimentation coefficients at much lower concentrations than those attainable with optical analytical ultracentrifugation. (Theoretically, one could set the loading concentration at about twice the lowest concentration recognizable by the analytical tool at hand, the only limiting factor being boundary stability.) But in polydispersity studies the situation is different. Since the final concentrations across the boundary can decrease by a practical factor of even 50 times when we move from the faster to the slower species, it is usually impossible to detect the whole range of concentrations if the initial value is already too low. In general, then, the loading concentration for polydispersity studies by the transport method needs to be higher than for a parallel determination of sedimentation coefficients by the same methodology. If this rise in concentration places the system at a level too far removed from what could be considered "zero" concentration then the extrapolation process cannot be avoided. This, of course, would be very laborious since it implies re-running all the set of determinations at different initial concentrations. A very good alternative is to use the procedure described by Baldwin (1954) in which knowledge of the dependence of s on concentration is the only requirement to do the extrapolation. This dependence can be found very easily by the transport technique, considering the high dilutions attainable as explained above.

In conclusion, it can be said that the experimental results of the present publication constitute a good proof that the nonoptical methodology of ultracentrifugal analysis based upon transport considerations can duplicate, with some loss of precision, the main operations and capabilities of conventional analytical ultracentrifugation, bringing to the ultracentrifugal field of analysis its own particular advantages: minute amounts, low concentrations, selective biological activity, and workability with crude preparations.

Acknowledgments

We gratefully acknowledge the support and encouragement of Dr. David S. Howell. We are indebted to Dr. Lawrence Rosenberg and Stanley W. Sajdera for their samples of highly purified preparations of proteoglycan complex and proteoglycan subunit, respectively. We also gratefully thank Dr. Lino G. Novoa for his mathematical assistance.

Appendix

$$\theta \equiv \frac{\pi s}{2\bar{s}} \tag{I}$$

$$g(s) = \frac{1}{\bar{s}} \sin^2\theta \tag{II}$$

$$G(s) = \frac{s}{2\bar{s}} - \frac{1}{2\pi} \sin 2\theta \tag{III}$$

$$\frac{C_F}{C_0} = \frac{x_m}{H}\left\{\frac{\bar{s}}{(\bar{s}\omega^2 t)^2 + \pi^2}\left[\omega^2 t \sin^2\theta + \frac{\pi}{\bar{s}} \sin\theta\cos\theta + \frac{\pi^2}{2\bar{s}^2\omega^2 t}(e^{2\omega^2 t} - 1)\right] + \frac{1}{2\pi} \sin 2\theta - \frac{Z}{2\bar{s}}\right\} \tag{IV}$$

$$\frac{C_F}{C_0} = \frac{Z}{4\bar{s}} - \frac{\bar{s}}{2\pi^2 Z}(1 - \cos 2\theta) \tag{V}$$

References

Baldwin, R. L. (1954), *J. Amer. Chem. Soc. 76*, 402.
Bitter, T., and Muir, H. M. (1962), *Anal. Biochem. 4*, 330.
Charlwood, P. A. (1952), *Biochem. J. 51*, 113.
Dische, Z. J. (1947), *J. Biol. Chem. 167*, 189.
Franek, M. D., and Dunstone, J. R. (1967), *J. Biol. Chem.*

242, 3460.
Hascall, V. C., and Sajdera, S. W. (1969), *J. Biol. Chem. 244*, 2384.
Hascall, V. C., and Sajdera, S. W. (1970), *J. Biol. Chem. 245*, 4920.
Howell, D. S., Pita, J. C., and Marquez, J. F. (1966), *Anal. Chem. 38*, 434.
Lowry, O. H., Rosebrough, N. J., Farr, A. L., and Randall, R. J. (1951), *J. Biol. Chem. 193*, 265.
Pita, J. C., and Müller, F. J. (1972), *Anal. Biochem. 47*, 395.
Rosenberg, L., Pal, S., Beale, R., and Schubert, M. (1970), *J. Biol. Chem. 245*, 4112.
Schachman, H. K. (1959), *in* Ultracentrifugation in Biochemistry, New York, N. Y., Academic Press, p 135.
Schack, I. A. (1965), *in* Industrial Heat Transfer, New York, N. Y., Wiley, p 35.
Schumaker, V. N., and Schachman, H. K. (1957), *Biochim. Biophys. Acta 23*, 628.
Svedberg, T., and Pedersen, K. A. (1940), *in* The Ultracentrifuge, Oxford, England, Clarendon Press, p 18.
Watanabe, I., Stent, G. S., and Schachman, H. K. (1954), *Biochim. Biophys. Acta 15*, 38.

Photochemical Systems of *Rhodospirillum rubrum*. Light-Induced Reactions and Biological Functions of *c*-Type Cytochromes in Relation to P-870†

William R. Smith, Jr., Christiaan Sybesma, William J. Litchfield, and Karl Dus*

ABSTRACT: Evidence from light-induced reactions, electrofocusing, amino acid analysis, and immunochemical characterization is presented to prove that cytochrome c_2 and cytochrome C-422 of *Rhodospirillum rubrum* are identical. The designation cytochrome c_2 also applies to the high-potential cytochromes of cyclic photochemical electron transport in *Rhodopseudomonas spheroides*, *Rhodopseudomonas viridis*, and *Rhodopseudomonas capsulata*, all of which can substitute for *R. rubrum* cytochrome c_2 by donating electrons to P-870 of *R. rubrum*. From light-induced reactions it is also suggested that cytochrome c' and the low-potential cytochrome C-428 of *R. rubrum* may be identical but no biological function can be assigned to this hemoprotein based on our studies. Only one photochemical system could be found to operate in *R. rubrum*, and this system appeared to be capable of oxidizing both the high-potential cytochrome c_2 and added cytochrome c'. However, no reaction of P-870 with the native cytochrome C-428 could be observed.

This study was undertaken with the aim to correlate the membrane-bound *c*-type cytochromes, C-422 and C-428 (Sybesma and Fowler, 1968), implicated in secondary electron-transport reactions in *Rhodospirillum rubrum*, with the chemically characterized, soluble cytochromes, c_2 and c', of this organism (Dus *et al.*, 1968; Kamen *et al.*, 1971; Kennel *et al.*, 1973). Furthermore, we intended to clarify the position of these cytochromes within the photochemical electron-transfer chain relative to the corresponding reaction center units and to scrutinize the concept of the possible existence of more than one type of reaction center in *R. rubrum* (Sybesma and Fowler, 1968; Fowler and Sybesma, 1970).

Previously, two photochemical systems were suggested to function in whole cells of *R. rubrum* (Sybesma and Fowler, 1968) based on different action spectra for the light-induced visible and near infrared absorbancy changes under continuous (Sybesma, 1969) and flashing (Sybesma and Kok, 1969) illumination. This was in agreement with action spectra of cytochromes C-555 and C-552 obtained by Morita (1968) in whole cells of *Chromatium vinosum* strain D which indicated oxidation of these cytochromes by different reaction centers. Measurements of the light-induced absorbancy changes as a function of redox potential in cells of *C. vinosum* strain D (Cusanovich *et al.*, 1968) and of *R. rubrum* (Fowler and Sybesma, 1970) led to similar conclusions. Specifically, in the experiments with *R. rubrum*, only one system, involving oxidation of cytochrome C-422 and interaction with the typical P-870 containing reaction center, seemed to operate under high-potential conditions. At potentials near zero, however, C-428, the low-potential cytochrome, was found to operate predominantly and the concomitant absorbancy changes in the near-infrared region were no longer those indicative of the typical P-870 containing reaction center. Among other changes, in this case, an increase of absorbancy was observed at 905 nm. A similar increase at 905 nm under low potential conditions had been found previously in *C. vinosum* strain D (Cusanovich *et al.*, 1968). This observation was taken to indicate the presence of a second reaction center component, P', thought to be associated with noncyclic photochemical electron transport and capable of oxidizing only the low-potential cytochrome. An alternate explanation was offered by Vredenberg *et al.* (1965) who suggested that these absorbancy changes may reflect a conformational change in the chromatophore membrane.

† From the Biochemistry Branch, Institute of Surgical Research, Fort Sam Houston, Texas 78234 (W. R. S.), the Biophysical Laboratory, Faculty of Science, Free University of Brussels, 1050 Brussels, Belgium (C. S.), and the Department of Biochemistry, University of Illinois, Urbana, Illinois 61801 (W. J. L. and K. D.). *Received February 8, 1973.* We gratefully acknowledge that these researches were supported in part by grants from the National Institutes of Health (GM 18902) to K. D. and the National Science Foundation (GB 30649X) to C. S., and by funds made available from the Biomedical Research Council of the University of Illinois.